Medical Technology (13:30 ～16:00 THP Seminar Room)

Session chairs: Prof. Shinya Wakusawa
Prof. Tsutomu Kawabe

Sleep disorder and sleep-disordered breathing in the elderly

C.Nakazaki[1)], A.Noda[2)], N.Fujita[3)], S.Yamada[1), 4)], Y.Koike[2)], S.Wakusawa[1), 4)]

1) Department of Pathophysiological Laboratory Sciences, Nagoya University Graduate School of Medicine, Nagoya, Japan
2) College of Life and Health Sciences, Chubu University
3) Department of Clinical Laboratory at Nagoya University Hospital
4) Department of Medical Technology, Nagoya University School of Health Sciences, Nagoya, Japan

Introduction

The elderly spend more time in bed, experience more awakenings during the night,[1)] and have increased complaints of sleep disorder such as the difficulty initiating sleep, difficulty remaining asleep and early morning awakenings.[2)] Elderly individuals complain primarily about sleep disorder, which are often secondary to other disorders. [1)]

Aging substantially increases the risk of obstructive sleep apnea syndrome (OSAS),[3)] and OSAS is associated with hypertension, cerebrovascular disorder, cardiovascular disease and all-cause mortality.[4)] However, effects of aging on pathophysiology of apnea/hypopnea in clinical settings have not been clearly investigated

We assessed the sleep disorder in middle-aged and elderly people, and examined the relation between sleep disordered-breathing (SDB) and cardiovascular function in the elderly.

Materials and Methods

Subjects: 32 middle-aged subjects (51.3±4.1 years, male: 16 subjects, female: 16 subjects) and 20 elderly (71.7±5.8 years, male: 5 subjects, female: 15 subjects) were targeted. The study protocol was approved by the appropriate institutional review committee at the Nagoya University, and informed written consent from the subjects was obtained at the beginning of the assessment.

Functional Outcome Measures: Subjective sleep symptoms, disturbances, and patterns were assessed with the Pittsburgh Sleep Quality Index (PSQI). The total global score ranges from 0 to 21, and greater scores indicate higher levels of sleep symptoms.[5)] Subjects with PSQI ≥ 6 were defined as insomnia. Daytime sleepiness was quantified using the Epworth Sleepiness Scale (ESS). Possible scores ranges from 0 to 24, and higher scores reflect greater sleepiness. A cut-off value ≥ 11 indicated excessive daytime somnolence (EDS) [6)].

Actigraphy: The actigraph (Ambulatory Monitoring, Inc, USA) was worn around the wrist of a non-dominant hand. The actigraph data were assessed using the algorithm supplied by the ActionW-2 clinical sleep analysis software package for Windows (Ambulatory Monitoring, Inc, USA). Sleep and activity were scored according to the Cole-Kripke formula.[7)] Total sleep time (TST) was measured using actigraphy.[8)]

Measurements for Sleep Apnea: To assess the sleep apnea, overnight examination was performed on each subjects using the portable home monitoring (apnomonitor: CHEST) and we calculated apnea-hypopnea index/h (AHI/h), oxygen desaturation index/h (ODI/h) and lowest arterial oxyhemoglobin saturation (Lowest SpO_2). We determined the subjects of AHI ≥ 5/h as sleep apnea syndrome (SAS).

Markers of Atherosclerosis: We evaluated atherosclerosis from Pulse Wave Velocity (PWV) and carotid ultrasonography. PWV was measured using a volume-plethysmographic (from PWV/ABI; Nihon Colin Co.,Ltd.,, Komaki, Japan), which simultaneously records brachial-ankle PWV (baPWV), blood pressure, an electrocardiogram, and heart sounds.[9)] The intima-media thickness (IMT) of the carotid arteries was estimated by B-mode ultrasound (HEWLETT PACKARD SONOS 2000 : PHILIPS) with a 7.5MHz. [10) 11), 12)]

Echocardiograph: Standard echocardiography including measurement of transmitral flow velocity indices (HEWLETT PACKARD SONOS 2000 : PHILIPS) was performed in all subjects. Left atrium dimension (LAD), left ventricular end-diastolic dimension (LVDd) and left ventricular end-systolic dimension (LVDs) were measured by two-dimensional M-mode, and the left ventricular ejection fraction (LVEF) was calculated. The peak early velocity (E) and atrium contraction velocity (A), their ratio (E/A) and the deceleration time of peak E velocity (DcT) were measured from mitral inflow velocities.

Data analysis: All statistical analyses were performed using a statistical software package (Statview for Windows version 4.54 SAS Institute Inc; Cary, NC). Data were presented by mean ± standard deviation (SD), and analysis of variance follow (ANOVA) by Scheffe's test was used to compare means of continuous values between subgroups. A probability (p) value < 0.05 were considered statistically significant.

Results

ESS was significantly higher in the middle-aged group than in the elderly group (8.1±5.1 vs 3.9±2.9, p=0.01). (Figure 1)

Bed time was significantly earlier in the elderly group than in the middle-aged group. (21:25±0.19 vs 22:59±0.17, p=0.019) There was no significantly difference between two groups in wake-up time. (Figure 2)

The prevalence of PSQI ≥ 6 (insomnia) was 45% in the elderly group, and it was 28% in the middle-aged group. In the elderly, Time in bed was significantly extended in the insomnia group than in the non-insomnia group. (8.6±1.6h vs 7.5±1.0h, p=0.038) (Table 1)

There were no significantly differences between SAS and non-SAS groups in atherosclerotic and echocardiographic parameters. (Table 2)

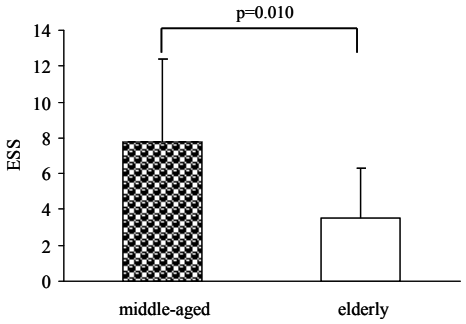

Figure 1. ESS between middle-aged and elderly group
ESS: Epworth Sleepiness Scale

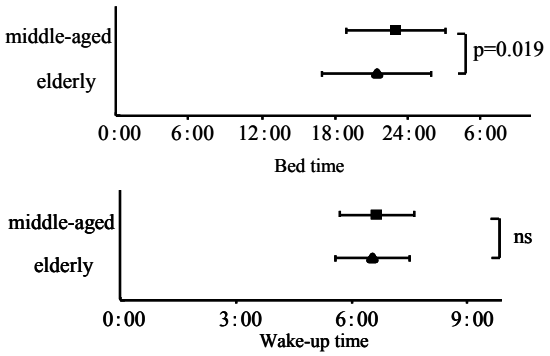

Figure 2. Bed time and wake-up time between middle- aged and elderly group

Table 1. Time in bed in the elderly group

	insomnia n=9	non-insomnia n=11	P value
PSQI	7.2±2.4	4.3±1.2	<0.001
Time in bed (hr)	8.6±1.6	7.5±1.0	<0.05

Data are presented as mean ± SD.
PSQI: Pittsburgh Sleep Quality Index

Table2 . Atherosclerotic and echocardiographic parameters in the elderly group

	SAS n=11	non-SAS n=9	P value
R-IMT Max (mm)	0.9 ± 0.4	1.1 ± 0.5	ns
L-IMT Max (mm)	0.9 ± 0.5	1.0 ± 0.3	ns
R-baPWV (cm/s)	1608.0 ± 382.0	1568.0 ± 285.0	ns
L-baPWV (cm/s)	1628.0 ± 300.0	1597.0 ± 256.0	ns
LVEF (%)	66.4 ± 6.1	70.0 ± 12.1	ns
E/A	0.8 ± 0.2	0.9 ± 0.3	ns
DcT (sec)	207.0 ± 36.5	210.0 ± 59.4	ns

Data are presented as mean ± SD.
IMT: intima-media thickness; baPWV: brachial-ankle pulse wave velocity; LVEF: left ventricular ejection fraction; E/A: peak early systolic velocity (E)/atrial contraction velocity (A); DcT: deceleration time of peak E velocity

Discussion

Epidemiological studies have implicated OSAS as a risk factor for the development of cardiovascular and cerebrovascular disease. However, in this study, cardiovascular function did not significantly differ between SAS and non-SAS groups in the elderly. Moreover, AHI did not significant change with a presence of hypertension or hyperlipidemia.

ESS score was significantly higher in the middle-aged group than in the elderly group, and bed time was significantly later. Daytime sleepiness was found in the middle-aged group and TST during the night was short. In the elderly, daytime sleepiness was not detected, but insomnia was permitted especially who spend long time in bed. Sleep disorder may relate to decrease of daytime activity and sleep quality.

In conclusion, comparison of sleep disorder/SDB and cardiovascular function between middle-aged and elderly population may provide insight into the pathophysiology of sleep disorder/SDB associated with aging.

References

[1] Sonia Ancoli-Israel, J. Steven Poceta, et al. Identification and treatment of sleep problems in the elderly. Sleep Med Rev 1997; 1: 3-17

[2] Ohayon MM, et al. Epidemiology of insomnia: what we know and what we still need to learn. Sleep Med Rev 2002; 6(2):97–111.

[3] Matthias E, Amy S. Jordan, Nancy L. Chamberlin, et al. The influence of aging on pharyngeal collapsibility during sleep. Chest 2007; 131: 1702-1709

[4] Heather E, David J, et al. Neuropsychological function in obstructive sleep apnoea. Sleep Med Rev 1999; 1: 59-78

[5] Buysse DJ, Reynolds CF, 3rd, Monk TH, et al. The Pittsburgh Sleep Quality Index: a new instrument for psychiatric practice and research. Psychiatry Res 1989; 28: 193-213

[6] Johns MW, et al. A new method for measuring daytime sleepiness: the Epworth sleepiness scale. Sleep 1991; 14(6); 540-545

[7] Cole RJ, Kripke DF, Gruen W, Mullaney DJ, Gillin JC: Automatic sleep/wake identification from wrist activity. Sleep 1992; 15: 461-469

[8] Van Den Berg JF, Van Rooij FJ, Vos H, et al. Disagreement between subjective and actigraphic measures of sleep duration in a population-based study of elderly persons. J Sleep Res. Sep 2008;17(3):295-302

[9] Yufu K, Takahashi N, Hara M et al. Measurement of the brachial-ankle pulse wave velocity and flow-mediated dilatation in young, healthy smokers. Hypertens Res 2007; 30(7); 607-612

[10] Kitamura A, Iso H, Imano H, et al. Prevalence and correlates of carotid atherosclerosis among elderly Japanese men. Atherosclerosis 2004; 172:353-359

[11] Renzhe Cui, Kitamura A, Yamagishi K, et al. Ankle-arm blood pressure index as a correlate of preclinical carotid atherosclerosis in elderly Japanese men. Atherosclerosis 2006; 184: 420-424

[12] Handa N, Matsumoto M, Maeda H, et al. Ultrasonic evaluation of early carotid atherosclerosis. Stroke 1990; 21; 1567-1572

Author address

E-Mail: nakazaki.chie@h.mbox.nagoya-u.ac.jp

Mycobacterium tuberculosis-induced expression of Granulocyte-Macrophage Colony Stimulating Factor is mediated by ERK1/2 MAPK or PI3-K/Akt signaling pathway

Jang-Eun Cho[1)], Sang-Jung Park[1)], Yong-Mi Kim[2)], Sang-Nae Cho[2)] , Hye-Young Lee[1)] and Yoon-Suk Kim[1)]

1) Department of Biomedical Laboratory Science, College of Health Sciences, Yonsei University, Wonju
2) Department of Microbiology, College of Medicine, Yonsei University, Seoul

Introduction

Mycobacterium tuberculosis, the causative agent of tuberculosis, has already infected nearly a third of the world's population causing approximately 2 million deaths yearly. Infection with MTB affects the recruitment and activation of circulating effector leukocytes by influencing induction and secretion of cytokines from infected macrophages. Infected macrophages release a variety of inflammatory cytokines as defense mechanisms against MTB. The cytokine GM-CSF plays an important role in the differentiation of monocytes, alveolar macrophages and dendritic cells. GM-CSF acts locally as a proinflammatory cytokine. In the lungs, GM-CSF is very important for macrophage maturation and differentiation and host defense. It was previously reported that GM-CSF can induce up-regulation of MHC class II and costimulatory molecules such as CD80 and CD86 on antigen presenting cells (APCs) as well as increasing their phagocytic activity and stimulatory capacity. When this cytokine is lacking, as in gene-disrupted mice, the architecture of the lung is altered and alveolar macrophages become foamy in appearance. In addition, these cells have defects in phagocytosis, bacterial killing, as well as loss of Toll-like receptor expression and signaling. In the context of tuberculosis, GM-CSF may also contribute to the cytokine/chemokine milieu responsible for granuloma formation in the lung. Over-expression of GM-CSF in the lungs impairs protective immunity against MTB and therefore careful regulation of pulmonary GM-CSF levels may be critical in sustaining protection against chronic tuberculosis disease. GM-CSF act as a pivotal factor for the development of alveolar macrophages in lung. Increasing GM-CSF levels into the chronic stage of the infection results in elevated cell proliferation and phagocytic activity. GM-CSF regulates both pulmonary surfactant homeostasis and the differentiation and proliferation of functionally competent alveolar macrophages. But the intracellular signaling pathways involved in the regulation of GM-CSF expression in alveolar macrophages are unclear. In this study, we aimed to elucidate the involvement of GM-CSF in the host immune response against MTB infection. We observed mycobacterium-stimulated induction of GM-CSF and evaluated the associated with signal transduction pathway.

Materials and Methods

Preparation of Mycobacteria

Mycobacterium tuberculosis H37Rv (ATCC 27294), M. bovis BCG (ATCC 35748) and clinical isolated Beijing family of MTB strain (K-strain) obtained at Yonsei Medical school in Seoul and used in this study was grown for about four weeks at 37°C as a surface pellicle on Sauton medium enriched with 0.4% sodium glutamate and 3.0% glycerol. The surface pellicles were collected and disrupted by gentle vortexing with 6mm glass beads. After clumps had settled, the upper suspension was collected and aliquots were stored at -80°C. Before infection, aliquots were thawed and quantitated for viable colony-forming units (CFU) on Middlebrook 7H10 agar (Difco, USA)..

Cell culture and infection of mycobacteria

THP-1 cell line was maintained in RPMI 1640 medium with 2 mM glutamine, 10% heat inactivated fetal bovine serum, 100 U/ml penicillin and 100 μg/ml streptomycin (Gibco-BRL, USA) at 37℃ under 5% CO2 condition. THP-1 cells were seeded in six-well plates and treated with 50 nM phorbol-12-myristate-13-acetate (PMA; Sigma) for 48 h to induce differentiation into macrophage-like cells, then washed three times with antibiotics free RPMI 1640 medium. Before infection, differentiated THP-1 cells were reconstituted in antibiotics free RPMI 1640 medium with 5% FBS. Cells were incubated with MTB at 10 MOI for 0, 1, 1.5, 3, 6, 9, 12, 18, 24, 48 or 72 h. PMA-differentiated THP-1 cells were pretreated with inhibitors for 45 min before stimulation with MTB H37Rv for 4 h at 10 MOI.

RNA extraction and Semi-quantitative RT-PCR

Total RNA was extracted from cultured cells using Trizol Reagent (Invitrogen, USA) according to the manufacturer's instruction. cDNA was synthesized by reverse transcription with 2 μg total RNA, 0.25 μg of random hexamer (Invitrogen) and 200 unit of Murine Molony Leukemia Virus Reverse Transcriptase (MMLV-RT; Invitrogen) for 10min at 25°C, 50min at 37°C and 15min at 70°C. Diluted reverse-transcribed cDNA was used subsequent 25 μl PCR amplification. PCR amplification using 0.2 units of G-Taq polymerase (Cosmo Genetech, Korea) was performed in a thermocycler (Applied Biosystems, USA) for 35 cycles using GM-CSF primer. GAPDH was ampilifed as an internal control. The intensity of each band amplified by RT-PCR was analyzed using Gel Doc EQ Quantity One (Bio-rad, Italy) and normalized to GAPDH mRNA in corresponding samples.

Enzyme-linked immunosorbent assay (ELISA)

Cell culture supernatants from MTB-infected THP-1 cells were collected 24 h after infection. Cell culture supernatants were analyzed using Human GM-CSF ELISA MAX™ Standard (BioLegend, USA), as recommended by the manufacturer.

Statistics

All values are given as mean ± standard deviation (SD). When a significant difference was detected, further analysis was performed using a Student's t-test. A p value of less than 0.05 was considered significant.

Results

MTB infected THP-1 cells induced a dose-dependent manner and a time-dependent increase in GM-CSF mRNA

Expression of GM-CSF was up-regulated by infection of MTB in a dose-dependent manner, reaching a peak at 20 MOI of MTB. We also examined the effects of mycobacterial infection on the timing of GM-CSF expression. GM-CSF expression was up-regulated in response to MTB in a time-dependent manner. The mRNA level of GM-CSF peaked at 6 h after mycobacterial infection, and then declined gradually for 72 h.

Induction of GM-CSF by MTB is mediated by p38 MAPK, ERK1/2 MAPK, PI3-K or PLC signaling pathway.

To elucidate the mechanism by which mycobacterial infection affects expression of GM-CSF, we determined the signaling pathway associated with MTB-stimulated induction of GM-CSF. Treatment with Ro-31-8425 (an inhibitor of calsscial PKC) or SP600125 (an inhibitor of JNK) did not influence of GM-CSF induction by MTB. SB202190 (an inhibitors of p38 MAPK), PD98059 (inhibitor of ERK1/2), Ly294002 (inhibitor of PI3-K) and U73122 (inhibitor of PLC) had negative effects on MTB-stimulated GM-CSF expression.

Mycobacterial infection induces GM-CSF secretion and the induction of GM-CSF by MTB is mediated by ERK1/2 MAPK or PI3-K/PDK1/Akt signaling pathway.

Differentiated THP-1 cells were pre-treated with indicated concentrations of PD98059 (ERK1/2 inhibitor), Ly294002 (PI3-K inhibitor), OSU03012 (PDK1 inhibitor) or Akt (Akt inhibitor IV) for 45 min, followed by MTB infection (10 MOI). Supernatants were harvested 24 h after infection and secretion of GM-CSF was measured by ELISA. All signal inhibitors were decreased GM-CSF secretion at high dose of specific signal inhibitors. PD98059 and Ly294002 decreased about 85 % of GM-CSF secretion, OSU03012 and Akt decreased about half of GM-CSF secretion.

Discussion

The Members of the CSF cytokine family play important roles in macrophage recruitment and activation to regions of inflammation. In mycobacterial infection, alveolar macrophage displays increasing levels of GM-CSF. However, mechanism of GM-CSF induction does not poorly understood. We investigated whether increasing levels of GM-CSF in mycobacteria infected THP-1 cell mediated mycobacterial secreted proteins. The increase in expression and secretion of GM-CSF was caused by MTB was reduced in cells treated with inhibitors of ERK1/2 MAPK. In addition the induction of GM-CSF caused by MTB was partially reduced in cells treated with inhibitors of p38 MAPK. In addition, the increase in secretion of GM-CSF caused by MTB was reduced in cells treated with inhibitors of PI3-K, PDK1 and Akt. These results suggest that GM-CSF plays important role in the immune response against mycobacterium infection. Therefore this signal transduction system might be a target for screeing therapeutic candidates for mycobacterial disease

References

[1]Szeliga J, Daniel DS, Yang CH, Sever-Chroneos Z, Jagannath C, Chroneos ZC. Granulocyte-macrophage colony stimulating factor-mediated innate responses in tuberculosis. *Tuberculosis*. 2008; 88; 7–20.

[2]North RJ, Jung YJ. Immunity to tuberculosis. Annu Rev Immunol. 2004;22;599–623.

[3]Fleetwood AJ, Cook AD, Hamilton JA. Functions of granulocyte–macrophage colony-stimulating factor. *Crit Rev Immunol*. 2005;25;405–28.

[4]Bonfield TL, Raychaudhuri B, Malur A, Abraham S, Trapnell BC, Kavuru MS, et al. PU.1 regulation of human alveolar macrophage differentiation requires granulocyte–macrophage colonystimulating factor. *Am J Physiol Lung Cell Mol Physiol*. 2003;285;L1132–6.

[5]Algood, H.M., Chan, J., and Flynn, J.L., Chemokine and tuberculosis. Cytokine Growth Factor Rev. 2003;14;467–477.

[6]Bozinovski S, Jones JE, Vlahos R, Hamilton JA, Anderson GP. Granulocyte/macrophage-colony-stimulating factor (GM-CSF) regulates lung innate immunity to lipopolysaccharide through Akt/Erk activation of NF-kappa B and AP-1 in vivo. *J Biol Chem*. 2002;277(45):42808-14.

Author address

E-Mail: hyelee@yonsei.ac.kr

MOLECULAR BASIS OF DECREASE OF PROTEIN S IN PREGNANCY: 17β-ESTRADIOL DOWN-REGULATES PROTEIN S (PS) EXPRESSION RECRUITING CO-REPRESSOR COMPLEX TO THE PS PROMOTER

A. Suzuki[1)], Y. Miyawaki[1)], J. Fujita[1)], A. Maki[1)], Y. Fujimori[1)], A. Takagi[1, 2)], T. Murate[1, 2)], H. Saito[3)] and T. Kojima[1, 2)]

1) Department of Pathophysiological Laboratory Sciences, Nagoya University Graduate School of Medicine, Nagoya, Japan
2) Department of Medical Technology, Nagoya University School of Health Sciences, Nagoya, Japan
3) Nagoya Central Hospital, Nagoya, Japan

Introduction

Anticoagulant Protein S (PS) is a vitamin K-dependent plasma protein that functions as a nonenzymatic cofactor for activated protein C in the anticoagulation pathway [1]. Decreased levels of plasma PS are known as a risk factor for the development of deep venous thrombosis, and there are many factors to cause the PS deficiency [2-4].

Hereditary PS deficiency is determined by detection of genetic mutation in PSα gene (*PROS1*) [5]. PS deficiency can also occur throughout life under the acquired conditions such as oral anticoagulant (i.e. warfalin) use and liver disease [6]. Furthermore, acquired PS deficiency has been reported in individuals with high levels of estrogen during pregnancy and in those taking oral contraceptives [7-9].

Estrogens are reported as the regulator of the specific gene expression via estrogen receptors [10]. The estrogen receptor (ER) is one of the steroid/nuclear receptor, and the ligand-bound ER functions as a transcriptional factor [11]. The classical ER action involves ligand-induced formation of an ER homodimer, which interacts with estrogen responsive elements (EREs) in target gene promoters [11]. The ligand-occupied ER is also known to associate with other transcription factors, not mediating EREs to modulate ligand-dependent gene expression [12-15].

In this study, we investigated the molecular basis of the PS decrease caused by E2, and thus the genomic ER signaling pathway modulating ligand-dependent *PROS1* gene repression, in HepG2-ERα cells stably expressing human ERα.

Materials and Methods

Establishment of HepG2-ERα cell line: HepG2 cells that stably express human ERα (HepG2-ERα) was established by G418 selection and used for further study.

Quantitative RT-PCR and ELISA: Quantitative reverse transcription (RT)-PCR was performed to determine PS mRNA and GAPDH mRNA using Power SYBR Green Master mix. Enzyme-linked immunosorbent assay (ELISA) was carried out to determine human PS antigen.

Luciferase Reporter Assay: To determine the *PROS1* promoter activity, luciferase reporter assay was performed in respective cell lines. Luciferase activity was normalized to the activity of co-transfected β-galactosidase.

Electrophoretic Mobility Shift Assay (EMSA), DNA Pull-down Assay and Chromatin Immunoprecipitation (ChIP) assay: EMSA and DNA pulldown assay were carried out to determine the transcription factors binding to the *PROS1* promoter regions using artificial double-stranded oligonucleotides. ChIP assay was performed with specific antibodies against various transcription factors bound intracellular DNA of the cells.

Results

PS expression was repressed by 17β-estradiol in human normal hepatocytes and HepG2-ERα cells: To determine the effect of 17β-estradiol (E2) to the *PROS1* expression, we analyzed PS mRNA in human normal hepatocytes (hNHeps) and HepG2 or its-derived cell lines. In ERα-positive hNHeps treated with 100nM E2, PS mRNA was decreased compared with vehicle-treated cells. In HepG2-ERα cells, PS mRNA and antigen were also repressed by E2 treatment, but not in ERα-negative other cell lines.

Down-regulation of PROS1 promoter activity by E2: To investigate of the effects on *PROS1* promoter activity, we cloned the promoter region of *PROS1* and constructed luciferase-reporter vectors. In the full-length promoter construct (PS-4229/pGL3) and its-truncated constructs (PS-1826/pGL3 to PS-175/pGL3), luciferase activities were down-regulated by E2, but PS-137/pGL3 was not. There are two adjacent GC-rich motifs between -175 and -137, and PS-175Mut/pGL3 containing mutations of these GC-rich motifs did not show E2-dependent repression.

ERα mediated E2-dependent PROS1 down-regulation: We also examined the necessity of ERα expression for the *PROS1* repression by E2 in HepG2-derived cells. In HepG2-mock transfected cells, the *PROS1* promoter activity was not down-regulated by E2 treatment, but was in HepG2-ERα cells. A pure ER antagonist, ICI 182,780, blocked this E2-induced *PROS1* repression.

Transcription factor Sp1, Sp3 and ERα bound to the PROS1 promoter region, and Sp1 was necessary for E2-dependent repression: Next, we performed the DNA pulldown assay and the electrophoretic mobility shift assay (EMSA) to identify the transcriptional factors interacted with the *PROS1* promoter. In DNA pulldown analyses, we found that Sp1, Sp3 and ERα bound to the oligonucleotide containing the GC-rich motifs of *PROS1* promoter. We also observed the bindings of Sp1 and Sp3 to the same oligonucleotide in EMSA, but could not detected ERα binding. To verify the functions of Sp proteins in the E2-induced *PROS1* repression, we carried out knockdown experiments for Sp1 and Sp3 by RNA interference using specific siRNAs against them. The knockdown of Sp proteins resulted in reduced promoter activities, but E2-dependent repression did not occur by knockdown of Sp1, whereas remaining E2-responsiveness by knockdown of Sp3.

Sp1/ERα interacted receptor interacting protein 140 (RIP140), and recruited co-repressor-HDAC complex: We performed the chromatin immunoprecipitation (ChIP) assay and ChIP re-immunoprecipitation (IP) assay to investigate the chromatin states of E2-treated HepG2-ERα cells. In ChIP assays, we observed the bindings of Sp1, Sp3 and ERα to the *PROS1* promoter region containing GC-rich motifs as well as DNA pulldown assay. Sp1 and Sp3 were bound to the GC-rich motifs

in an E2-independent manner, but Sp1 binding was enhanced by E2 treatment. The binding of ERα was completely in an E2-dependent manner. In further analyses of transcription factors interacting with the *PROS1* promoter, we found that co-repressor nuclear receptor co-repressor (NCoR) and silencing mediator of retinoid and thyroid hormone receptors (SMRT) were E2-dependently recruited to the GC-rich motifs. These co-repressors were not known to be recruited by liganded ERα, however, we tried ChIP assays for receptor interacting protein 140 (RIP140) [16] and ligand-dependent co-repressor (LCoR) [17], which are known to interact liganded ERα, and we identified only RIP140 bound to the *PROS1* promoter containing GC-rich motifs. Because RIP140 is also known to interact histone deacetylases (HDACs) [18], we investigated the recruitment of them. We observed class I HDAC; HDAC3 was robustly recruited by E2-treatment, whereas class II HDACs did not affected.

To confirm the interaction of these transcription factors upon the *PROS1* promoter region containing GC-rich motifs, we performed ChIP re-IP assays. The results suggested that Sp1 interacted ERα, and Sp1/ERα recruited NCoR/SMRT-HDAC3 complex via RIP140. A HDAC inhibitor trichostatin A (TSA) blocked E2-dependent repression, so *PROS1* gene repression was mediated HDACs, which induced a hypo-acetylated chromatin state and less permissive transcription.

Discussion

The decreased level of plasma PS during pregnancy is a well-known risk factor for deep venous thrombosis, but its precise mechanism has not been unknown. In this study, we clarified that PS decrease was induced by 17β-estradiol through transcriptional repression.

Meanwhile, the action of estrogen has been investigated well, which is ligand-dependent modulation of estrogen receptor and regulation of transcription in target gene. Although the positive regulation of target gene expression by estrogen receptor has been reported in various studies, negative regulation of target gene expression has been less understood. Especially, liganded ER had been thought to only regulate the transcription positively. We identified liganded ER has a potential of negative regulation, mediating RIP140 and co-repressor-HDAC complex. RIP140 is known to interact HDACs, whereas HDACs exist sometimes as complex such as NCoR/SMRT-HDAC, so there might be another formation accompanied with ER-RIP140 upon the target gene promoter.

In the down-regulation of protein S gene expression, the interaction of Sp1 and ERα might be important. The Sp1 formed complex with ERα upon the GC-rich motifs of the *PROS1* promoter, and consequently they reinforced the stability of Sp1/ERα-DNA complex. The interacted ERα recruited RIP140, and RIP140 recruited the NCoR/SMRT-HDAC3 complex. The NCoR/SMRT-HDAC3 complex might induce the hypoacetylated histones, in which DNA could coil tightly and limited accessibility of the basal transcription factors and thus repressing the *PROS1* expression.

Conclusions

In this study, we have demonstrated that 17β-estradiol down-regulates protein S gene expression via ERα. Liganded ERα interacts basal transcriptional factor Sp1 and recruits RIP140, which associates directly with HDAC3 complex containing NCoR and SMRT. Thus E2-dependent *PROS1* repression results in decreased levels of plasma PS, and this leads to the risk of deep venous thrombosis during pregnancy or oral contraceptive use.

References

[1] Dahlbäck, B. (1991) *Thromb Haemost* **66**, 49-61
[2] Schwarz, H. et al, (1984) *Blood* **64**, 1297-1300
[3] Engesser, L. et al. (1987) *Ann Intern Med.* **106**, 677-682
[4] Makris, M. et al. (2000) *Blood* **95**, 1935-1941
[5] Gandrille, S. et al. (2000) *Thromb Haemost.* **84**, 918
[6] D'Angelo, A. (1988) *J Clin Invest.* **81**, 1445-1454
[7] Comp, P. et al. (1986) *Blood* **68**, 881-885
[8] Malm, J. et al. (1988) *B J Haematol* **68**, 437-443
[9] Tans, G., et al. (2000) *Thromb Haemost* **84**, 15-21
[10] Hall, J. et al. (2001) *J. Biol. Chem.* **276**, 36869-36872
[11] Gruber, C. et al. (2002) *N Engl J Med* **346**, 340-352
[12] Delfino, F. et al. (1999) *Mol Cell Endocrinol* **157**, 1-9
[13] Kushner, P. J. et al. (2000) *J Ster Biochem Mol Biol* **74**, 311-317
[14] Levin, C. (2005) *Eur J Nuclear Med Mol Imaging* **32**, S325-S345
[15] Safe, S. et al. (2004) Nuclear Receptor-Mediated Transactivation Through Interaction with Sp Proteins. in *Progress in Nucleic Acid Research and Molecular Biology*, Academic Press. pp 1-36
[16] de Wolf, C. J. et al. (2006) *J Biol Chem* **281**, 17635-17643
[17] Safe, S., and Kim, K. (2008) *J Mol Endocrinol* **41**, 263-275
[18] Owen, G. et al. (1998) *J Biol Chem.* **273**, 10696-10701

Author address

E-Mail: suzuki.atsuo@d.mbox.nagoya-u.ac.jp

COMPARISON OF REBA HPV-ID® WITH DNA CHIP BASED ASSAY FOR HPV GENOTYPING

Sung-Hyun Kim[1)*], Dong-Sup Lee[2)*], Sang-Jung Park[1)], Tae-Ue Kim[1)], Gwang-Hwa Park[2)], and Hye-Young Lee[1)]

1) Department of Biomedical Laboratory Science, College of Health Sciences, Yonsei University

2) Department of Pathology, College of Medicine, Yonsei University Wonju Christian Hospital,

Wonju-si, Gangwon-do, Republic of Korea

Introduction

Human papillomaviruses(HPV)have been known to cause human cervical cancer which is the second most common cancer among women worldwide and the most common cancer among women in developing countries [1, 6, 9].

Even though, the HPV prevalence among subgroups of people classified by disease severity varies, overall prevalence of HPV in people with cervical cancer has been reported to reach up to 95 to 100% [9]. So far, more than 100 genotypes of HPV have been known. Among those, certain groups of HPV have been implicated to have high association with cervical cancer, whereas other types have low association [2]. In detail, the most associated geno-types with malignant cervical cancer are 16, 18, 45, 31, 33, 52, 58, and 35. Of these, HPV16 and 18 are mostly related to the malignant cervical cancer [1].

For this reason, HPV genotyping rather than mere detection of HPV has been recommended and thus, the test volume for HPV genotyping has been rapidly increasing. Nowadays, reliable and accurate detection method that able to identify the specific HPV genotypes is required, thus several PCR-based assays have been developed to detect specific genotypes of HPV [8]. Currently, many genotyping tests kits in clinical settings have been commercially available and evaluated to be valuable for clinical diagnosis [3, 8].

This study was set to evaluate a new HPV genotyping kit, REBA HPV-ID®from M&D (Wonju, Korea) for its usefulness for genotyping HPV using clinical specimens.

Materials and Methods

HPV samples and liquid based cytological smears

The clinical specimens were obtained since November of 2008 to July of 2009 using by standard procedure from 356 women in Gangwon province, Korea from Yonsei university Wonju Christian Hospital.

Cytological diagnosis

The Liquid-based cytological smears obtained using recommended procedures and clinical diagnoses were interpreted by the pathologists and were classified by 2001 Bethesda System terminology.

HPV genotyping

HPV genotyping using REBA HPV-ID® (M&D, Wonju, Korea) and MyHPV DNA Chip (Mygene, Seoul, Korea) were carried out according to the manufacturer's recommendation. Both genotyping methods, REBA HPV-ID® and MyHPV DNA Chip require the target region (firstly, amplify MY11 and MY9 then, amplify GP5 and GP6) amplification before performing the examination. After amplification of target region by PCR, post PCR steps performed according with manufacturer's recommendation. Briefly, for REBA HPV-ID® assay, PCR products added to the genotype specific probe labeled membrane strips, washed non-specific binds, and then stained with staining solution of PCR product-probe linked region of strips. For MyHPV DNA Chip assay, PCR product loaded to the probe labeled glass chip and then read the result signal using by scanner.

Sequencing

Total eight samples were analyzed by sequencing for conformational test. These eight samples have got positive result which appear single HPV genotype infection with REBA HPV-ID®, however the result was negative with MyHPV DNA Chip. For sequencing analysis, one-tube nested PCR was performed to amplify the target region (GP5 and GP6) and then, sequencing analysis was performed at Xenotech (Dae-joen, Korea).

Results

Clinical diagnosis of HPV

According to the cytological interpretations, 180 specimens (50.56%) were normal, 162 specimens (45.5%) were abnormal, and 14 specimens (3.93%) have not been diagnosed because which were prescribed to perform HPV genotyping directly without cytological diagnoses. Abnormal cytological diagnoses were classified 6 grades. Respectively, 67 (18.82%) ASCUS, 2 (0.56%) ASC-H, 50 (14.04%) LSIL, 30 (8.42%) HSIL, 12 (3.37%) SCC, and 1 (0.28%) C□B2C.

Genotyping of HPV in abnormal cytology, REBA HPV-ID® versus MyHPV DNA chip

The overall positivity of REBA HPV-ID® was 80.86% (186) using clinical specimens with abnormal cytological interpretation: the positivity rate of HPV with abnormal cytology was 91.67% (11) in SCC, 96.66% (29) in HSIL, 92% (46) in LSIL, 100% (2) in ASC-H, and 64.17% (43) in ASCUS. When the results from REBA HPV-ID® were compared with MyHPV DNA Chip, the overall positivity rate of MyHPV DNA chip was 69.75%, and the positivity rate of HPV with abnormal cytology was 91.67% (11) in SCC, 96.88% (29) in HSIL, 84 % (42) in LSIL, 100% (2) in ASC-H, and 43.28% (29) in ASCUS with MyHPV DNA chip. The positive rate of HPV in ASCUS was significantly lower with MyHPV DNA chip than with REBA HPV-ID®. These data shows that REBA HPV-ID® has about 30% higher sensitivity than MyHPV DNA chip.

The five most frequently detected HPV sub-types using REBA HPV-ID® were HPV16, 53, 58, 56, and 33 with abnormal cytological diagnosis, while using Mygene DNA chip,

HPV subtypes 16, 58, 56, 53, and 18 were most frequently detected.

Genotyping of HPV in normal cytology, REBA HPV-ID® versus MyHPV DNA chip

On the other hand, the rate of HPV positive was 64.44% (116) in REBA HPV-ID® and, 34.44% (62) in MyHPV DNA chip based assay with normal cytology. The data shows REBA HPV-ID® has about 2 fold higher positivity than DNA chip with normal cytological diagnosis. In this study, The five most remarkable HPV sub-types detected were HPV16, 53, 58, 18, and 56 with normal cytological diagnosis using REBA HPV-ID® and HPV16, 52, 18, 53, and 58 using MyHPV DNA chip. These data suggest that REBA HPV-ID® has higher specificity than MyHPV DNA chip.

Sequencing analysis with specimens that have different results

To confirm the accuracy and reliability of two methods, sequencing analysis was performed. Before the sequencing analysis, sorting of suitable specimens was required. Total seven specimens, which have negative results with MyHPV DNA Chip, have a strong signal of PCR and have single genotype infection result (one-band) with REBA HPV-ID®, were selected. GP5, GP6 region was amplified and sequenced. Five out of seven samples sequenced clearly to interpret data and these results were corrected with REBA HPV-ID® because these samples had negative results with MyHPV DNA Chip. The rest two samples could not be interpreted by sequencing analysis. They would be mixed infection which infected with more than two genotypes of HPV or non-HPV infection (negative). Therefore, these data suggest that REBA HPV-ID® has higher sensitivity (72.42%) and accuracy than MyHPV DNA Chip (28.57%).

Discussion

In this study, we evaluated the performance of the REBA HPV-ID® system which based on reverse blot hybridization assay compare with the results of DNA chip assay and cytological interpretation with clinical specimens.

Recently available HPV genotyping kit REBA HPV-ID® has several advantages over a DNA chip based HPV genotyping method. First of all, REBA does not require expensive equipments such as scanner. Second, it is more suitable for the laboratory with large volume of tests by saving labor and reducing turn-around time. The total time required for the REBA HPV-ID® was from PCR to genotyping analysis was about 4 hours. In brief, it can be more economical and time consuming.

According to our finding, the positivity of the REBA HPV-ID® was higher (80.86%) than other DNA chip based method (69.75%) in abnormal cytological samples and also positivity of REBA HPV-ID® (64.44%)was higher than MyHPV DNA chip (34.44%) in normal cytological samples. Thus, it seems that REBA HPV-ID® would provide more sensitive and specific detection rate for samples with abnormal and normal cytology.

To confirm the reliability of REBA HPV-ID®, Sequencing analysis was performed. Sequencing results show that REBA HPV-ID® was more reliable and higher sensitivity.

Conclusions

Sequencing analysis has a limitation that is not a golden standard method as a confirmative test because if some patients who infected with more than 2 HPV genotypes, the results could not be interpreted clearly. Therefore, other kinds of confirmative tests are required for accurate HPV genotype detection and need to further evaluation.

References

[1] Bosch F X, Lorincz A, Munoz N, Meijer C J and Shah K, The causal relation between humanpapillomavirus and cervical cancer. J. Clin. Pathol. 2002; 55 244–265.

[2] De Villiers EM, Fauquet C, Broker TR, Bernard HU, Zur Hausen H, Classification of papilloma-viruses. Virology 2004; 324:17-27.

[3] Fatima Galan-Sanchez, M A Rodriguez-Iglesias, Comparison of human papillomavirus genotyping using commercial assays based on PCR and reverse hybridization methods. APMIS 2009; 117: 708–15.

[4] F X Bosch, A Lorincz, N Muñoz, C J L M Meijer, K V Shah, The causal relation between human papillomavirus and cervical cancer. J. Clin. Pathol. 2004; 55:244–265.

[5] Roden R, Wu T C, How will HPV vaccines affect cervical cancer? Nat. Rev. Cancer. 2006; 6:753–763.

[6] Schiffman MH, Bauer HM, Hoover RN, Glass AG, Cadell DM, Rush BB(1993) Epidemiologic evidence showing that human papillomavirus infection causes most cervical intraepithelial neoplasia. J. Natl. Cancer. Inst. 1993; 85:958–64.

[7] S R Hong, I S Kim, D W Kim, M J Kim, A R Kim, Y O Kim, H S Kim, Prevalence and genotype distribution of cervical human papillomavirus DNA in Korean women : a multicenter study. Kor. J. Pathol. 2009; 43:342-50.

[8] Thomas Iftner, Liesje Germ, Ryan Swoyer, Development and clinical evaluation of a highly sensitive PCR-reverse hybridization line probe assay for detection and identification of anogenital human papillomavirus. J. Clin. Microbiol.1999;37:2508–2517.

[9] Walboomers, J. M. M., M. V. Jacobs, M. M. Manos, F. X. Bosch, A. Kummer, K. V. Shah, and P. J. F. Snijders. Human papillomavirus is a necessary cause of invasive cervical cancer worldwide. J. Pathol. 1999; 189:12–19.

Corresponding Author address

E-Mail: Hyelee@yonsei.ac.kr

Morphometric and FISH Analyses of Adenocarcinoma and Mesothelial Cells Using Liquid-Based Cytology

A.Morimoto[1)], T.Nagasaka[1), 2)], K.Hashimoto[1), 2)], T.Yokoi[3)]

1) Department of Pathophysiological Laboratory Sciences, Nagoya University Graduate School of Medicine, Nagoya, Japan
2) Department of Medical Technology, Nagoya University School of Health Sciences, Nagoya, Japan
3) Department of Diagnostic Pathology, Aichi Medical University Hospital, Nagakute, Aichi, Japan

Introduction

Cytological diagnosis of malignant effusions is often difficult mainly because of the presence of reactive mesothelial cells. The evaluation of cellular morphology with conventional Papanicolaou or Giemsa stains tend to be more or less subjective as shown by the interobserver and even the intraobserver variabilities. Immunocytochemistry has been applied to aid the differentiation of adenocarcinoma and reactive mesothelial cells, but is not very useful largely because of the limitation of the specimen. LBC is superior to conventional cytology in that it provides smear slides with a uniform cell density and a distribution that enables a precise cytological examination. Moreover, one can preserve cells in the LBC solution for a long period of time and always utilize it for a variety of purposes, such as immunocytochemistry and molecular analysis. To establish a more objective diagnostic system, we performed morphometric and FISH analyses on adenocarcinoma and mesothelial cells, using a liquid-based cytology method, and evaluated its usefulness.

Materials and Methods

Fourty five tumors of alimentary tract, 20 gastric adenocarcinomas and 25 colonic adenocarcinomas, were studied. Cells were harvested from the surface of tumor and serosa of resected fresh specimen, suspended in the solution for fixation and preservation (Liqui-PREP^{TM} Preservative Solution), and processed for Papanicolaou staining and FISH. Digital images were taken from Papanicolaou-stained slides for the following measurements. The nuclear area and perimeter of 100 cells per each case were measured using the software ImageJ (NIH), and the mean nuclear area (NA), the mean nuclear perimeter (NP), the mean length of nuclear longer axis (LLA) and their standard deviations (SNA, SNP, SLLA) were calculated. The shape factor (SHF) was obtained by the following formula: $(4\times \pi \times \text{area})/\text{perimeter}^2$. SHF is dimensionless and its value is equal to 1.0 in circles and <1.0 in spheroid nuclei (Figure 1). Standard deviations of the shape factor (SSHF) were also calculated. FISH analysis was performed to detect chromosome 8 polysomy and c-myc amplification.

Results

The nuclear area (NA) was smaller in gastric adenocarcinoma cells than in colonic adenocarcinoma cells and mesothelial cells, although the differences were not statistically significant. Results of the standard deviation of nuclear area (SNA) demonstrated that adenocarcinoma cells had more variable-sized nuclei than mesothelial cells (**P<0.01) (Figure 2).

Results of the nuclear perimeter (NP) showed a similar tendency to NA. As for the standard deviation of nuclear perimeter (SNP), colonic adenocarcinoma cells showed the highest value, followed by gastric adenocarcinoma cells, and mesothelial cells showed the lowest value (**P<0.01) (Figure 2).

As for the length of nuclear longer axis (LLA), colonic adenocarcinoma cells had longer nuclei (*P<0.05, **P<0.01) than gastric adenocarcinoma cells or mesothelial cells without a significant difference between the latter two. Results of the standard deviation of length of nuclear longer axis (SLLA) showed a similar tendency to SNP (**P<0.01) (Figure 2).

As for the shape factor (SHF), mesothelial cells had the most rounded nuclei, followed by gastric adenocarcinoma cells, and nuclei of colonic adenocarcinoma cells were the least rounded (**P<0.01). Results of the standard deviation of shape factor (SSHF) showed a similar tendency to SNP and SLLA (**P<0.01) (Figure 2).

Adenocarcinoma cells of both stomach and colon in all cases showed significant percentages of chromosome 8 polysomy and c-myc amplification, whereas mesothelial cells in all cases showed normal cell pattern.

Discussion

Morphometric analysis revealed that gastric adenocarcinoma cells were less atypical and more uniform than colonic adenocarcinoma cells and had even smaller nuclei than mesothelial cells. One should always take these facts into consideration on cytological examination, since gastric and colonic adenocarcinoma cells are definitely the most frequently encountered atypical cells in intraoperative peritoneal washing cytology, although cellular atypia should be more integratedly assessed using other indices. By FISH analysis using LBC specimens, quantitation of positive signals was more easily performed than with histology sections, resulting in detection of chromosome 8 polysomy and c-myc amplification in significant percentages of both gastric and colonic adenocarcinoma cells, whereas all the mesothelial cells showed the normal pattern.

Conclusions

Morphometric and FISH analyses, together with conventional stains and immunocytochemistry, using LBC method can be used as ancillary techniques in differentiation of adenocarcinoma and mesothelial cells.

Acknowledgment

The author is grateful to Dr. Akihiro Ito, Toki General Hospital, for providing clinical materials and Prof. Tsutomu Kawabe, Nagoya University School of Health Sciences, for reviewing the manuscript and giving useful advice.

References

[1]Bernstein SJ, Sanchez-Ramos L, Ndubisi B. Liquid-based cervical cytologic smear study and conventional Papanicolaou smears: a metaanalysis of prospective studies comparing cytologic diagnosis and sample adequacy. Am J Obstet Gynecol 2001;185:308-17.

[2]Nasuti JF, Tam D, Gupta PK. Diagnostic value of liquid-based (Thinprep) preparations in nongynecologic cases. Diagn Cytopathol 2001;24:137-41.

[3]Ikeguchi M, Oka S, Saito H, Kondo A, Tsujitani S, Maeta M, Kaibara N. Computerized nuclear morphometry: a new

morphologic assessment for advanced gastric adenocarcinoma. Ann Surg 1999;229:55-61.
[4]Susumu N, Aoki D, Noda T, Nagashima Y, Hirao T, Tamada Y, Banno K, Suzuki A, Suzuki N, Tsuda H, Inazawa J, Nozawa S. Diagnostic clinical application of two-color fluorescence in situ hybridization that detects chromosome 1 and 17 alterations to direct touch smear and liquid-based thin-layer cytologic preparations of endometrial cancers. Int J Gynecol Cancer 2005;15:70-80.
[5]Koide K, Sakakura C, Hagiwara A, Yamaguchi T, Yamagishi H, Abe T, Inazawa J. An improved rapid procedure for fluorescence in situ hybridization that is applicable to intraoperative cancer cytodiagnosis. Cancer Lett 2000;158:165-9.

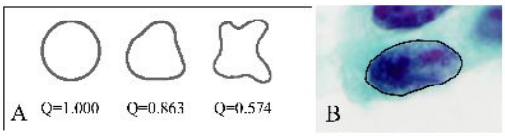

Figure 1. A: The shape factor (SHF) is dimensionless and its value is equal to 1.0 in circles and <1.0 in spheroid nuclei. B: The shape factor (SHF) of this picture shows 0.743, the nuclear area (NA) is 84.065 μ m^2, the nuclear perimeter (NP) is 37.700 μ m, and the length of nuclear longer axis (LLA) is 14.183 μ m.

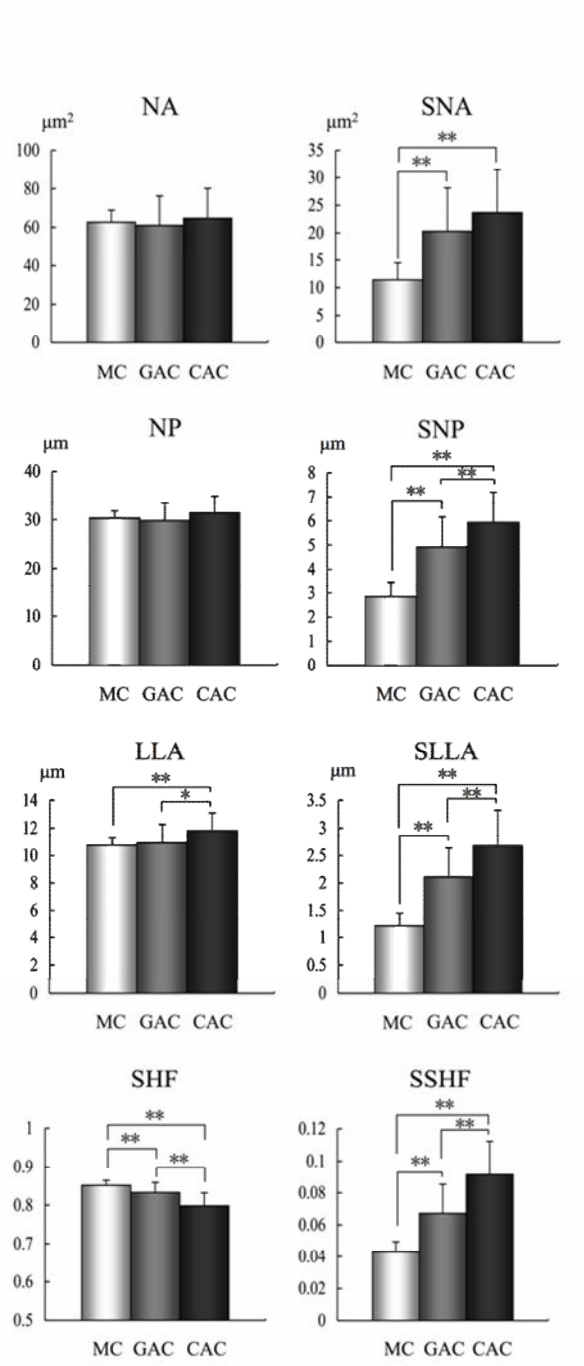

Figure 2. Results of morphometric analysis of mesothelial cells and adenocarcinoma cells on LBC slides. MC: mesothelial cells, GAC: gastric adenocarcinoma cells, CAC: colonic adenocarcinoma cells.

Author address
E-Mail: morimoto.ayumi@b.mbox.nagoya-u.ac.jp

MOLECULAR MECHANISM OF CERAMIDE KINASE GENE REPRESSION ON ATRA-INDUCED NEURONAL DIFFERENTIATION

Masashi Murakami[1), 2)], Hiromi Ito[2)], Kazumi Hagiwara[2), 3)], Noriko Sasaki[2)], Misa Kobayashi[2)], Asuka Hoshikawa[2)], Akira Takagi[2)], Tetsuhito Kojima[2)], Keiko Tamiya-Koizumi[4)], Yoshiko Banno[5)], Yoshinori Nozawa[6)], Takashi Murate[2), 7)]

1) Research Fellow of the Japan Society for the Promotion of Science, 2) Department of Pathophysiological Laboratory Sciences, Nagoya University Graduate School of Medicine, Nagoya, Japan, 3) National Hospital Organization, Nagoya Medical Center, Nagoya, Japan, 4) Division of Molecular Pathology, Aichi Cancer Center, Nagoya, Japan, 5) Department of Cell Signaling, Gifu University Graduate School of Medicine, Gifu, Japan, 6) Gifu International Institute of Biotechnology, Kakamigahara, Japan, 7) Department of Medical Technology, Nagoya University School of Health Sciences, Nagoya, Japan

Introduction

Ceramide kinase (CERK) is the enzyme that phosphorylated ceramide to ceramide 1-phosphate (C1P).

Previous studies suggested that ceramide kinase (CERK) and its product, ceramide 1-phosphate (C1P) have been implicated in various cellular function including cellular proliferation, survival, mast cell degranulation, and phagocytosis.

However, the regulatory mechanism of CERK gene expression remains to be determined.

In the current study, we examined the regulatory mechanism of CERK gene expression during all-*trans* retinoic acid (ATRA)-induced neuronal differentiation of a human neuroblastoma cell line, SH-SY5Y cells.

Materials and Methods

Cell line: A human neuroblastoma cell line, SH-SY5Y, was cultured in Dulbecco's Eagle's medium supplemented with 10% fetal bovine serum.

Establishment of CERK stable transfectants: Human CERK cDNA was the kind gift of Dr. Kohama T. (Daiichi-Sankyo Co., Ltd., Tokyo, Japan). hCERK cDNA was inserted into pcDNA3.1(+) expression vector (Invitrogen, California, USA). To establish the stable transfectants of CERK, DNA transfection was performed by the calcium precipitation method. A subclone (sc 17) showing the highest CERK protein expression was used for further experiments.

Cell proliferation and cell death: Cell proliferation was determined in triplicate with WST-1 assay kit (Roche Applied Science, Mannheim, Germany). Cell death was determined with LDH-cytotoxic test (Wako Pure Chemical Industry, Osaka, Japan).

CERK enzyme activity: CERK activity was determined as described previously [1] with some modification.

Western blotting: Western blotting was performed using ECL plus western blotting system (Amersham Pharmacia Biotech, Buckinghamshire, UK).

Quantitative RT-PCR: Quantitative RT-PCR was performed as described previously [2]. The primers were as follows: CERK sense 5'-AGTCCACCACAACAGCAC-3', antisense 5'-GAGGAAGGTCTTTAAACCTG-3', Sphingosine kinase 1 (SPHK1) sense 5'-TCCTGGCACTGCTGCACTC-3', antisense 5'-TAACCATCAATTCCCCATCCAC-3', and GAPDH sense 5'-CAGGAGCGAGATCCCTCCAA-3', antisense 5'-CCCCCTGCAAATGAGCCC-3'.

Cloning of the 5'-promoter region of human CERK: Human CERK 5'-promoter region was prepared using a PCR-based method. Using suitable restriction enzymes, this promoter region was inserted into pGL3 Basic vector (Promega, Madison, USA). The deletion mutants were prepared using Exonuclease III digestion, PCR-based cloning, and restriction enzymes digestion method. To introduce the mutation to the RARE like motif, overlap extension PCR method was performed.

Luciferase assay: SH-SY5Y cells were plated at a density of $5x10^5$cells/ml in 35mm dishes. After 2 days of incubation, 0.5μg of promoter construct and 2μg of β-galactosidase expression vector were co-transfected into cells using lipofectin reagent (Invitrogen) according to the manufacturer's protocol. Luciferase activity and β-galactosidase activity were measured according to the method described previously [3].

Electrophoresis mobility shift assay (EMSA): EMSA was performed as described previously [4]. One μg of nuclear extract and 600 fmol of biotin-labeled probe were incubated at room temperature for 40 min. Cold probe was used for the competition experiment (x20 excess). For the supershift experiments, anti-RARα antibody, anti-RXRα antibody, and anti-COUP-TFI antibody (Santa Cruz) were used.

DNA pull-down assay: Nuclear extract, biotin-labeled double strand probe and Poly dI-dC were incubated in DNAP buffer for 30min on ice. Following the incubation, Dynabeads M-280 streptavidin (Invitrogen Dynal AS, Oslo, Norway) were added and mixed with rotator at 4°C for 30 min. Prior to this step, the beads were washed in DNAP buffer for 10 min with rotator at three times. After washing, dissolved in SDS sample buffer and heated at 95°C for 5 min. Western blotting was performed using anti-RARα, anti-RXRα, and anti-COUP-TFI antibody.

Chromatin immunoprecipitation assay (ChIP assay): ChIP assay was performed as described previously [4]. For immunoprecipitation, normal IgG, anti-RARα, anti-RXRα, anti-COUP-TFI, anti-N-CoR, anti-SMRT, and anti-HDAC3 antibody (Santa Cruz) were added to the lysate. The CERK promoter region was amplified by PCR using the following primer set. Sense: 5'-GTCCCCTCCGCGGTCCCC-3', antisense: 5'-GCTTCACCCACAGCACGGATT-3'.

Transient transfection followed by co-immunoprecipitation: The plasmids of RARα, RXRα, and COUP-TFI were the gift of Dr. W. H. Miller (McGill University, Quebec, Canada), Dr. R.M. Evans (The Salk Institute for Biological Studies, CA, USA), and Dr. G. Salbert (Universite de Rennes I, Rennes, France), respectively. After transfection with respective plasmid DNA using lipofectin reagent (Invitrogen), SH-SY5Y cells were treated with either ATRA or methoprene acid, a specific agonist of RXRα, for 24 h. Co-Immunoprecipitation assay was performed by described previously [5] with some modification.

Results

ATRA reduced CERK enzyme activity, CERK protein, and mRNA expression whereas another sphingolipid metabolic

enzyme, SPHK1 that had similar function to CERK, did not show significant changes with ATRA.

To examine transcriptional regulation of ATRA-induced CERK gene repression, promoter analysis was performed.

ATRA reduced CERK promoter activity, and this reduction was mainly because of the region between -40 and -28 bp from the first exon. In this region, the tandem retinoic acid responsive element (RARE) like motifs were identified with one base space. Introduction of mutation into these RARE like motifs, erased ATRA-induced inhibition of CERK promoter activity.

To determine which transcription factor was bound in these RARE like motifs, EMSA, DNA-pull down assay, and ChIP assay were performed.

These experiments revealed that ATRA induced binding of retinoic acid receptor α (RARα), retionid X receptor α (RXRα), Chicken ovalbumin upstream promoter transcription factor I (COUP-TFI) to these RARE like motifs. Moreover, ChIP assay showed that HDAC3, N-CoR, and SMRT were recruited to these RARE like motifs.

Transient expression of RARα, RXRα, and COUP-TFI and siRNA transfection of these genes concluded that COUP-TFI inhibited CERK mRNA.

Another ATRA-induced differentiation model, human acute myeloblastic leukemia cell line, HL60 cells, showed some increase of CERK mRNA with ATRA. Interestingly, ATRA induced binding of RARα and RXRα to these RARE like motifs, but COUP-TFI didn't.

These results suggested that the relative ratio of RAR/RXR and COUP-TFI/RXR or COUP-TFI/RAR might determine the level of CERK transcription in different cell lines.

To examine a function of CERK on cell proliferation, cell death, and neuronal differentiation of SH-SY5Y cells, we established stable transfectants of CERK. CERK over-expression counteracted ATRA-induced inhibition of cell proliferation and cell death under the serum starvation. On the contrary, siRNA of CERK enhanced the effect of ATRA on cell growth and cell death.

Furthermore, to examine the effect of neuronal differentiation, ATRA-induced neurite extension and growth associated protein-43 (GAP-43) protein expression, which was main component of growth cone, was examined. CERK over-expression inhibited ATRA-induced neuronal differentiation. On the contrary, siRNA of CERK enhanced neuronal differentiation.

These results revealed that CERK promoted cell proliferation and cell survival, and had an inhibitory effect against ATRA-induced neuronal differentiation.

Discussion

Recent analysis revealed that sphingolipid and their metabolic enzymes were involved in cellular signalling, cell survival, and cell death. CERK and its product, C1P have also been suggested to play an important role of cell survival and inflammation [6, 7]. Intriguingly, CERK is mainly distributed in brain, especially, highly expressed in cerebellum [8].

Our results of stable transfectants of CERK and siRNA of CERK not only confirmed previous results but also revealed CERK as the unique modulator of neuronal cell function in SH-SY5Y cells. It is very interesting that further analysis of elucidating the function of CERK in central nervous system.

We recently reported that SPHK1 gene expression was increased during glial-cell line derived neurotrophic factor (GDNF) induced neuronal differentiation of human neuroblastoma cell line, TGW cells [9]. But in ATRA-induced neuronal differentiation of SH-SY5Y cells, SPHK1 expression didn't show any change. This result suggested that CERK and SPHK1 play non-overlapping roles in neuronal differentiation.

Vitamin A and its major metabolite, ATRA, are essential for network formation during early brain development [10]. COUP-TFI involvement in modulating ATRA-induced differentiation has been reported in multiple cell types [11, 12]. Our results suggested that COUP-TFI modulated ATRA-induced CERK expression, and the possible role of CERK in the early physiological process of normal neuronal differentiation.

Conclusion

CERK is antagonistic to ATRA-induced neuronal differentiation and that a tandem RARE like motifs located in the 5'-promoter region was responsible for ATRA responsiveness, and found that COUP-TFI induced with ATRA treatment was responsible for CERK gene repression.

References

[1]Bajjalieh SM, Martin TF, Floor E. Synaptic vesicle ceramide kinase. A calcium-stimulated lipid kinase that co-purifies with brain synaptic vesicles. *J. Biol. Chem.* 1989;264:14354-14360.

[2]Sobue S, Iwasaki T, Sugisaki C, *et al*. Quantitative RT-PCR analysis of sphingolipid metabolic enzymes in acute leukemia and myelodysplastic syndromes. *Leukemia* 2006;20:2042-2046.

[3]Nakade Y, Banno Y, T-Koizumi K, *et al*. Regulation of sphingosine kinase 1 expression by protein kinase C in a human leukemia cell line, MEG-O1. *Biochim. Biophys. Acta* 2003;1635:104-116.

[4]Sobue S, Hagiwara K, Banno Y, *et al*. Transcription factor specificity protein 1 (Sp1) is the main regulator of nerve growth factor-induced sphingosine kinase 1 gene expression of the rat pheochromocytoma cell line, PC12. *J. Neurochem.* 2005;95:940-949.

[5]Lee HK, Park UH, Kim EJ, Um SJ. MED25 is distinct from TRAP220/MED1 in cooperating with CBP for retinoid receptor activation. *EMBO J.* 2007;26:3545-3557.

[6]Gomez-Munoz A, Kong JY, Parhar K, *et al*. Ceramide-1-phosphate promotes cell survival through activation of the phosphatidylinositol 3-kinase/protein kinase B pathway. *FEBS Lett.* 2005;579:3744-3750.

[7]Mitsutake S, Kim TJ, Inagaki Y, *et al*. Ceramide kinase is a mediator of calcium-dependent degranulation in mast cells. *J. Biol. Chem.* 2004;279:17570-17577.

[8]Mitsutake S, Yokose U, Kato M, *et al*. The generation and behavioral analysis of ceramide kinase-null mice, indicating a function in cerebellar Purkinje cells. *Biochem. Biophys. Res. Commun.* 2007;363:519-524.

[9]Murakami M, Ichihara M, Sobue S, *et al*. RET signaling-induced SPHK1 gene expression plays a role in both GDNF-induced differentiation and MEN2-type oncogenesis. *J. Neurochem.* 2007;102:1585-1594.

[10]Ross SA, McCaffery PJ, Drager UC, De Luca LM. Retinoids in embryonal development. *Physiol. Rev.* 2000;80:1021-1054.

[11]Beland M, Lohnes D. Chicken ovalbumin upstream promoter-transcription factor members repress retinoic acid-induced Cdx1 expression. *J. Biol. Chem.* 2005;280:13858-13862.

[12]Zhuang Y, Gudas LJ. Overexpression of COUP-TFI in murine embryonic stem cells reduces retinoic acid-associated growth arrest and increases extraembryonic endoderm gene expression. *Differentiation* 2008;76:760-771.

Author address

E-Mail: murakami.masashi@c.mbox.nagoya-u.ac.jp